UHECR: PROBLEMS and SOLUTIONS

V. Berezinsky

Gran Sasso Science Institute and Laboratori Nazionali del Gran Sasso

SPECTRA and EXPERIMENTS

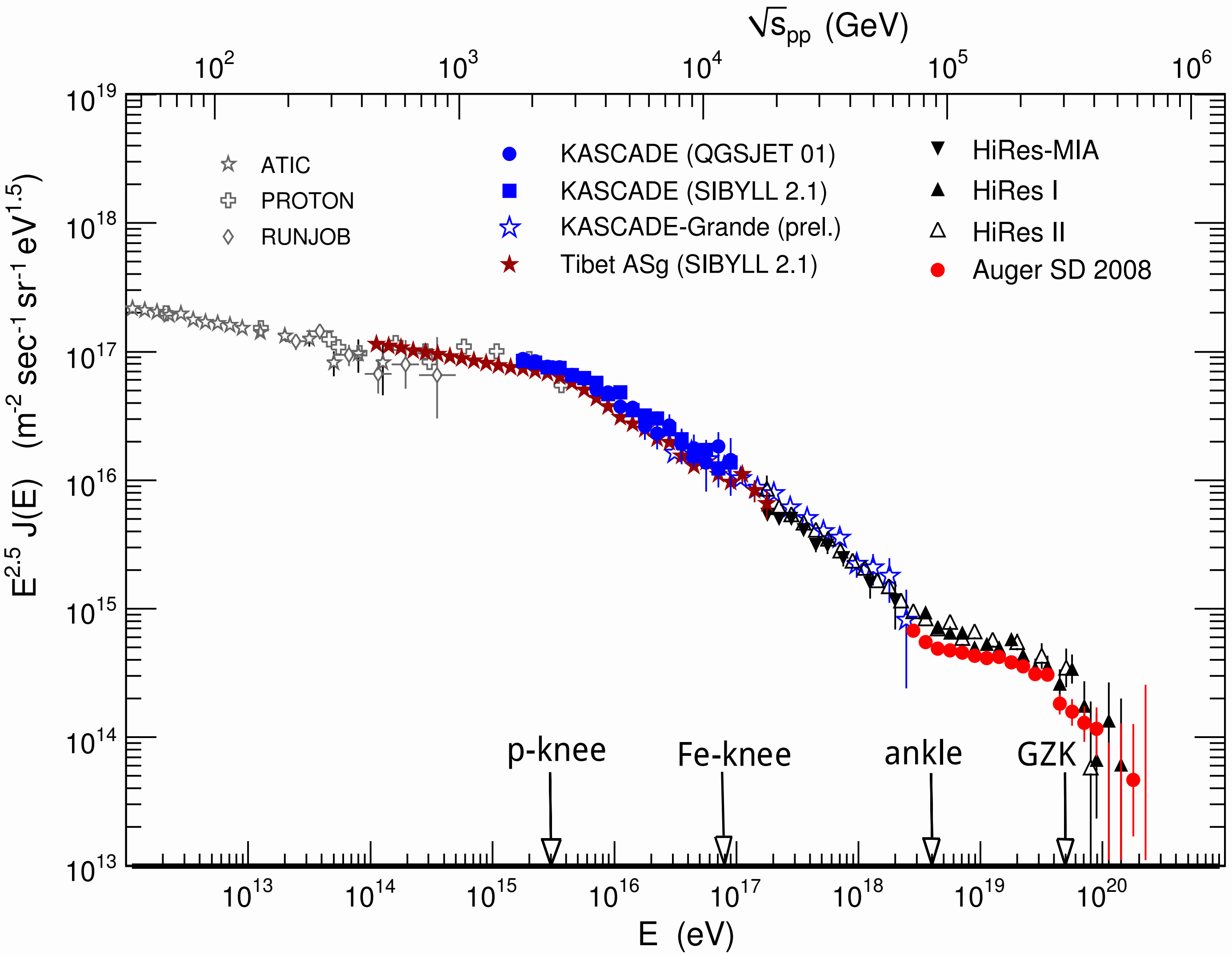

New technique: fluorescent light detection. calorimetric measurements.

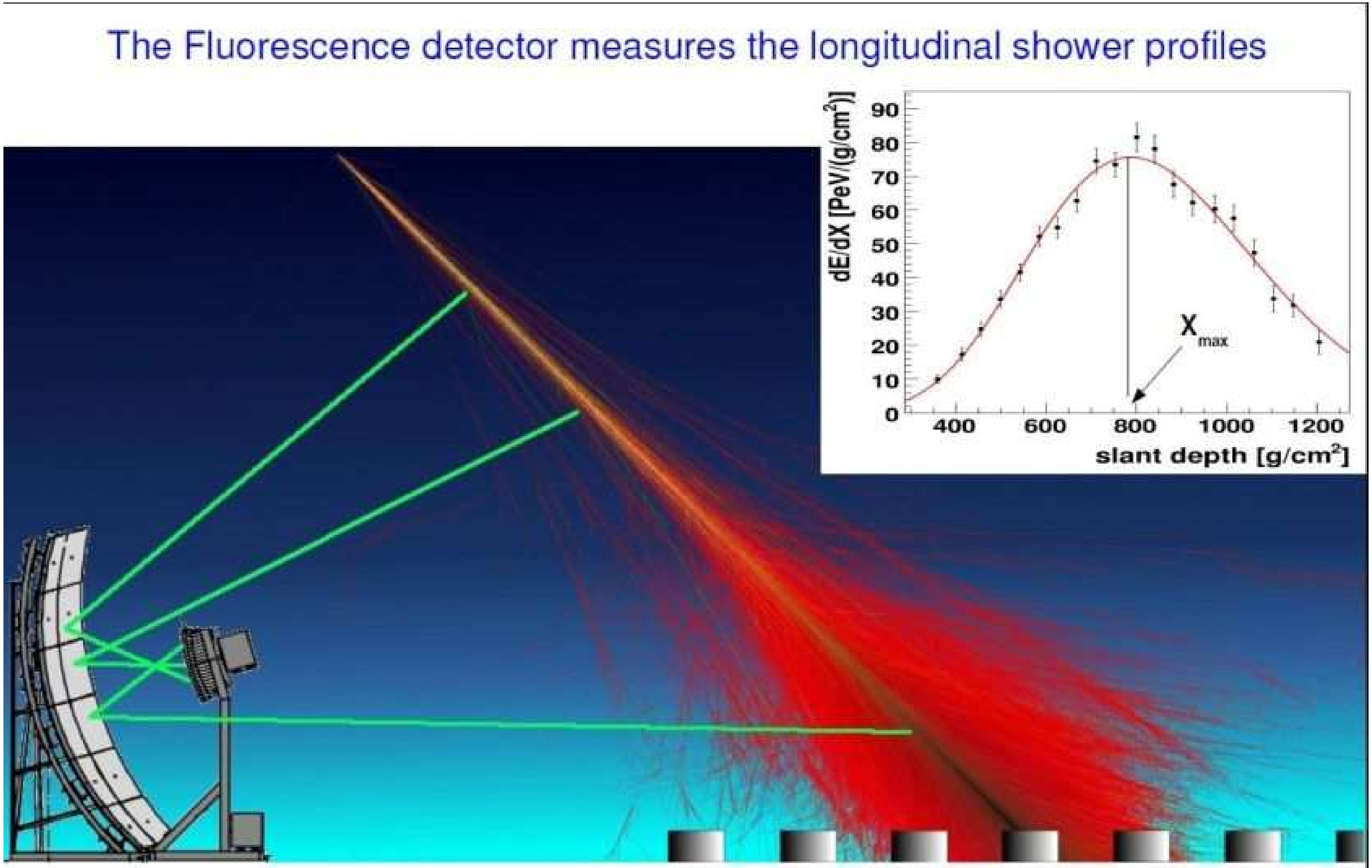

Last generation of UHECR detectors $10^{18} - 10^{20}$ eV.

- **FE and HiRes, the first fluorescent-light detectors with stereo observation.**
- **Pierre Auger Observatory (3000 km^2),**
  24 fluorescence detectors (4 sites), 1660 on-ground water-Cherenkov detectors, measurement of muon flux.
- **Telescope Array (680 km^2),**
  3 sites of fluorescent detectors, the biggest Middle Drum with 14 telescopes and 51 m^2 errors, and 507 scintillation detectors.
- **Future EUSO detectors:**
  space detectors of fluorescent light from Earth atmosphere.

EUSO PROJECTS

JEM-EUSO with d=2.5m mirror and KLYPVE-EUSO with segmented d=11m mirror.

PRINCIPLES OF EUSO OBSERVATIONS

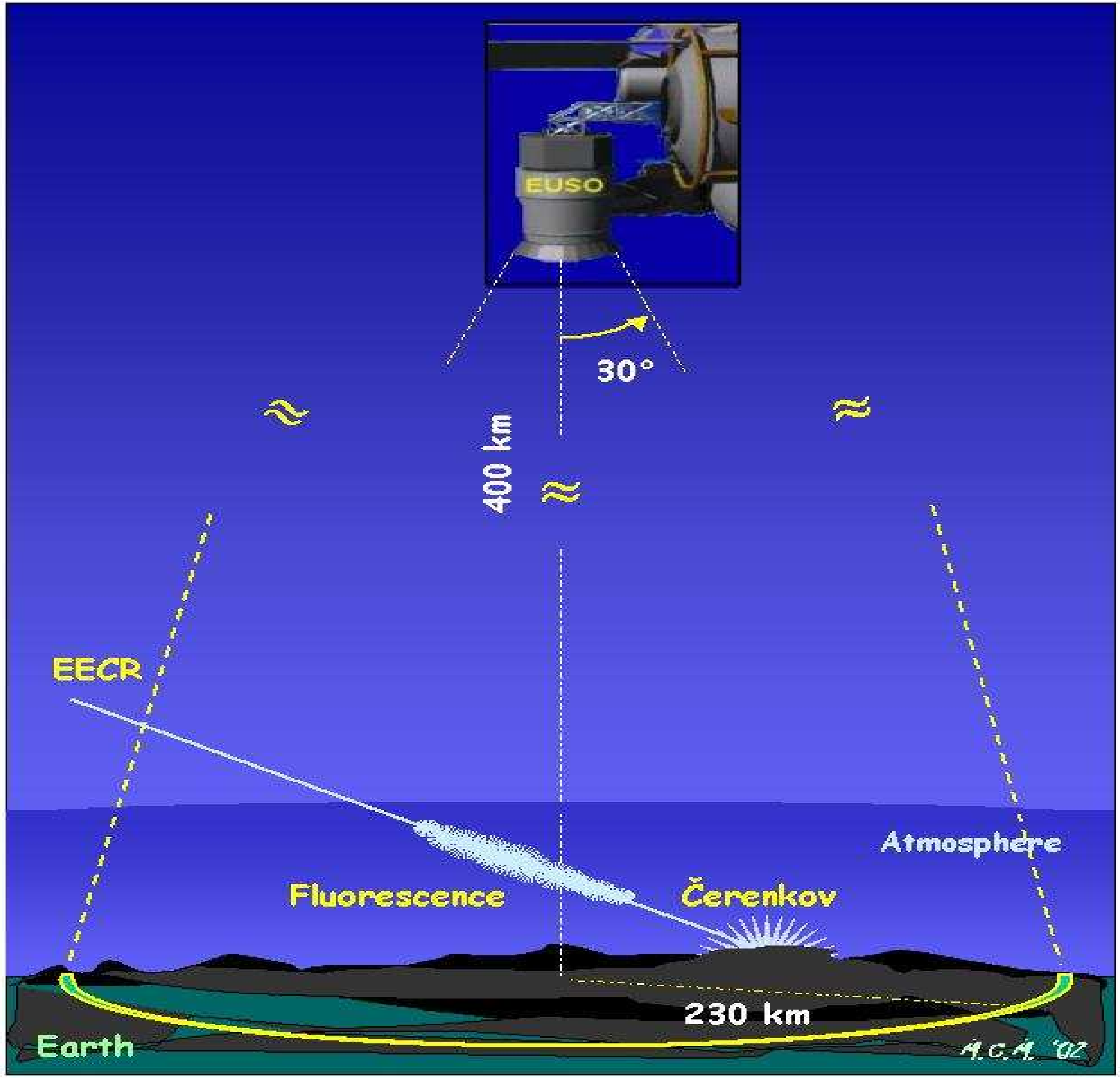

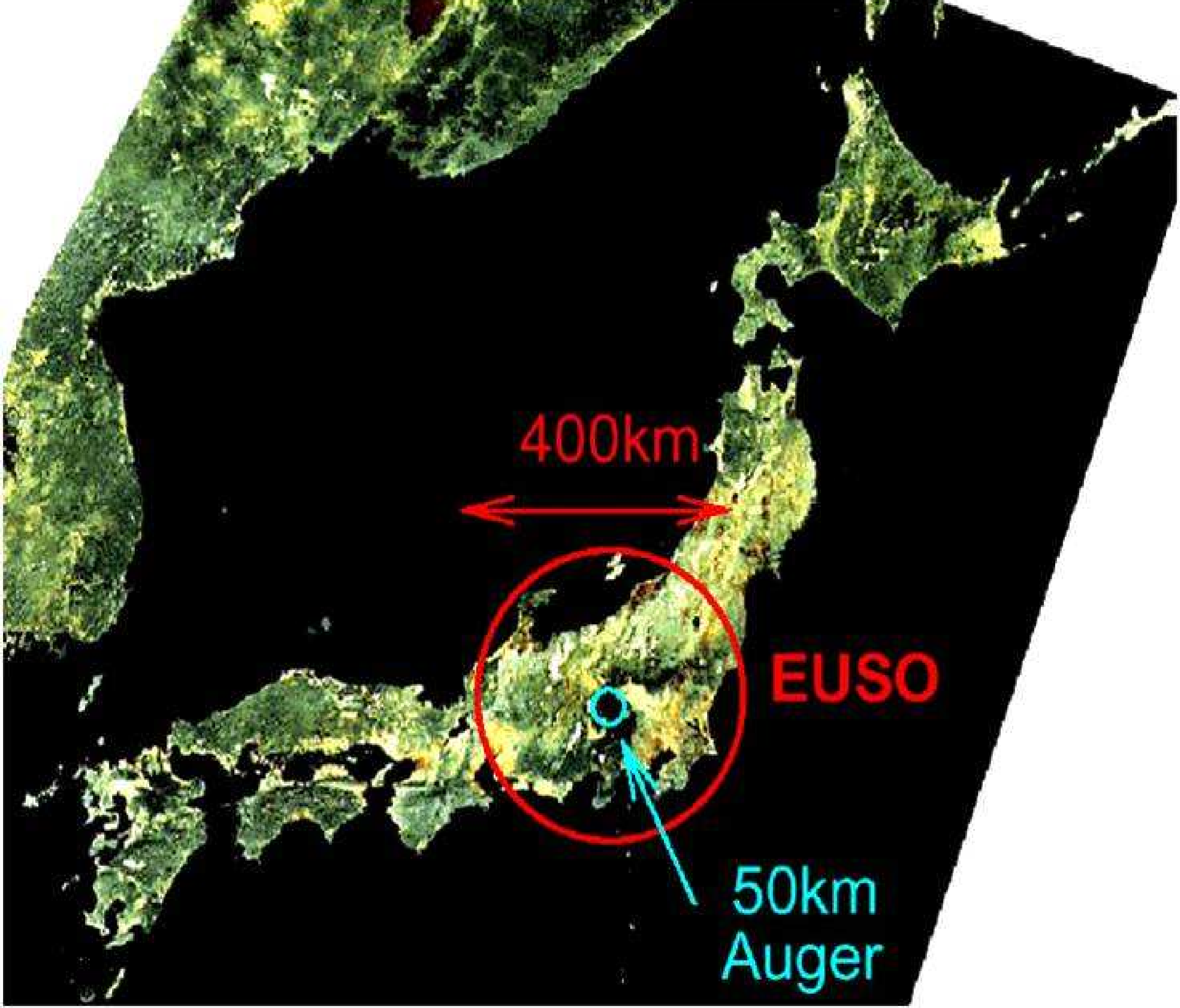

400km
EUSO
50km
Auger

GENERATION OF UHE ENERGY PARTICLES

UHE particles with energies up to $E \sim 10^{20}$ eV can be produced by acceleration:
e.g. shock acceleration, unipolar induction, strong electromagnetic waves
and by cosmological relics
in particular by Topological Defects and by Superheavy Dark Matter particles.

These particles can be observed as UHECR and neutrinos, in some cases as subdominant component.

$E_{\max}$ for non-relativistic jets (FR galaxies).

Biermann and Strittmatter 1987, Norman, Melrose, Achtenberg 1995, Ptuskin, Rogovaya, Zirakoshvili, 2013, (Blandford, Znajek 1977)

$E_{\max}$ from two conditions:
$E_{\max} = ZeBR_s$ (Hillas criterion) and
$B^2/8\pi = \omega_{\rm part}$ or $B^2/8\pi \approx L/\pi R_s^2 c\beta$ (equipartition), results in

$$E_{\max} \sim Ze(8L/c)^{1/2} \sim 6 \times 10^{19} Z L_{45}^{1/2}\ \text{eV} \quad (1)$$

for $\beta \sim 1$. Eq. (1) does not depend on $r_{\rm sh}$ and R_s.
Problem: At $\Gamma_j \lesssim 4$ jets are short, and HE protons are absorbed due to $p\gamma$ interaction.

Fanaroff-Riley I and II radio-galaxies

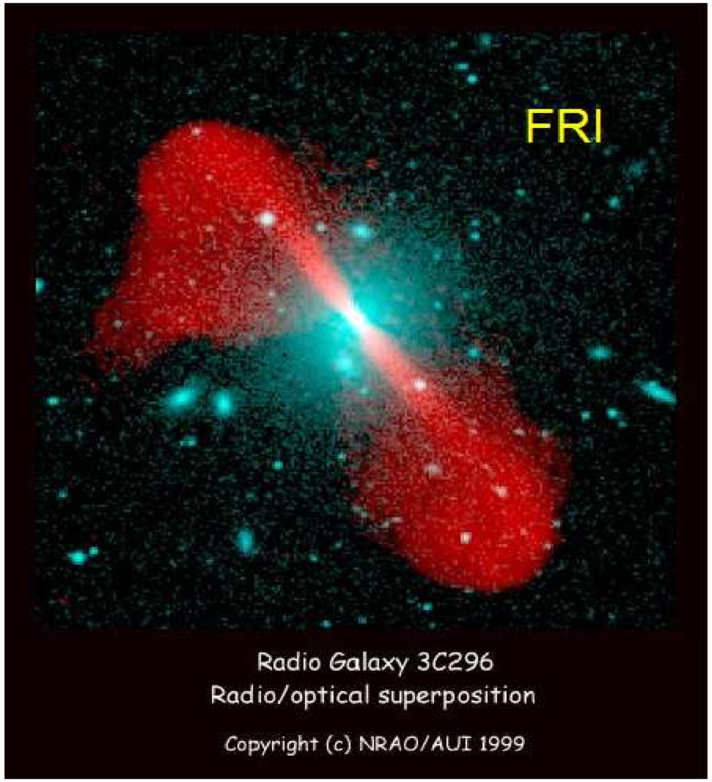

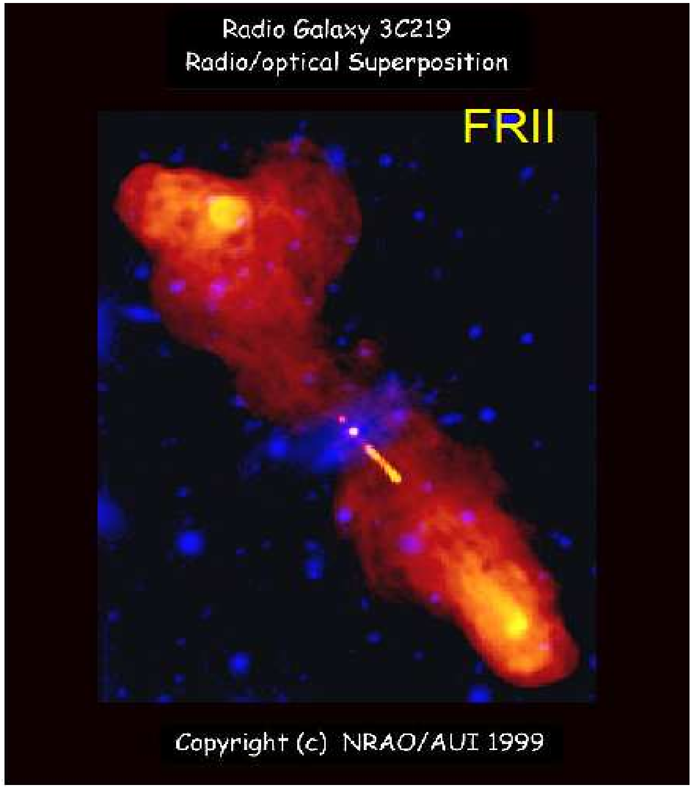

ACCELERATION IN RELATIVISTIC SHOCKS

looks very promising because at reflection a particle obtains $E \sim \Gamma_{\rm sh}^2 E_i$

Illustrative picture

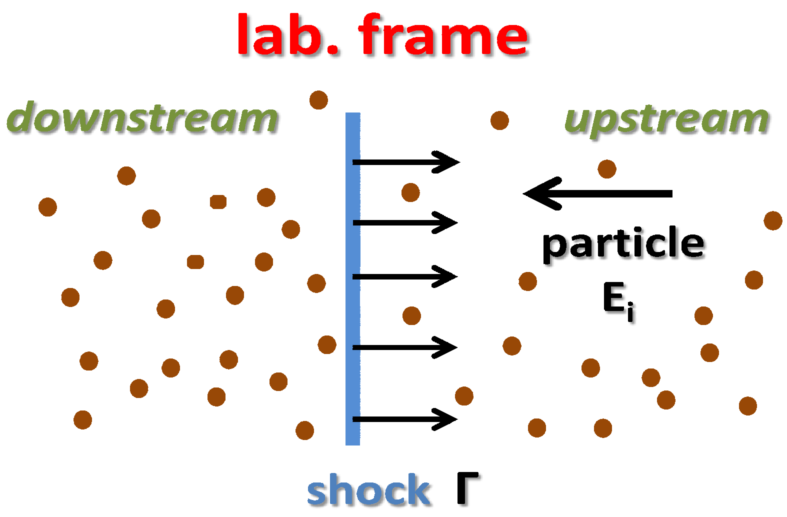

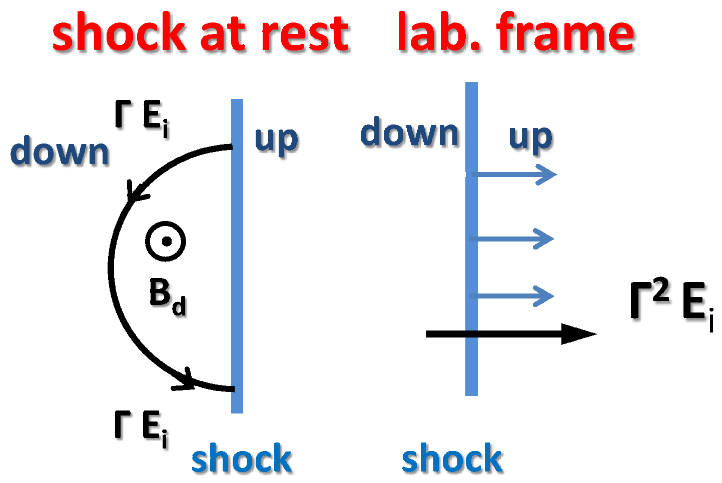

Problems

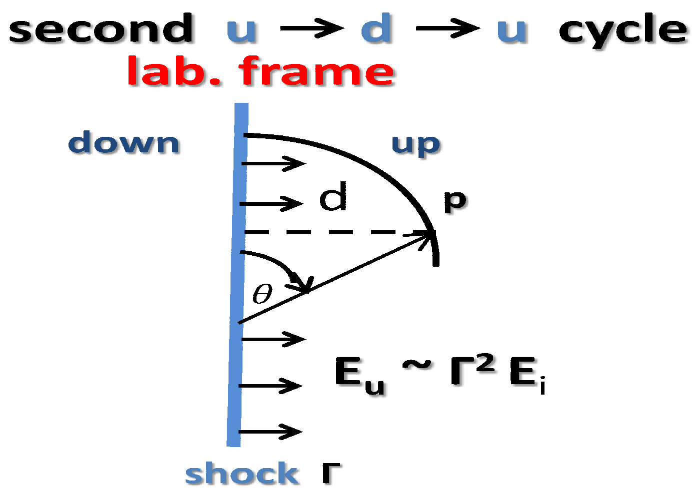

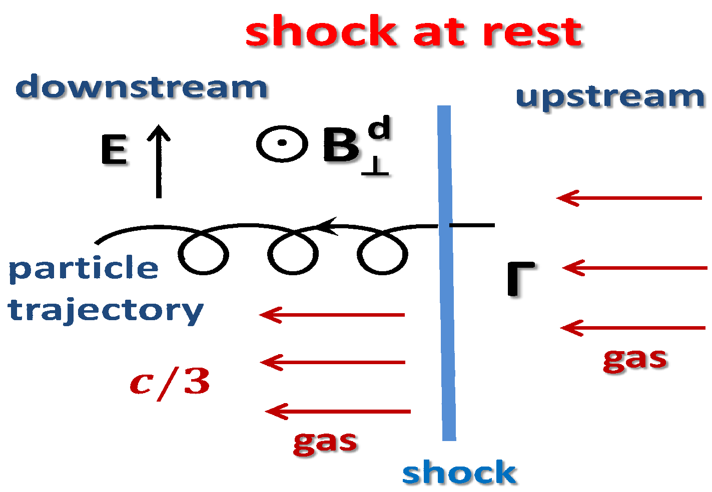

*

Revival

- **Self-generated streaming (Weibel) instability results in the production of microturbulence (Spitkovsky 2008, Sironi and Spitkovsky 2011).**
- **Repeating transition between upstream and downstream the Fermi regime is caused by scattering on these small-scale microturbulence.**
- **The scale of microturbulence is given by $\lambda \sim c/\omega_{pp}$ and acceleration takes place in weakly magnetised plasma $\sigma \sim \frac{B^2}{4\pi n m_p c^2} \ll 1$. (Lemoine and Pelletier 2010 - 2024, Bykov et al 2012, Reviille and Bell 2014).**

unHappy end: B. Reville and A.R. Bell 2014

When times of two competing processes, isotropisation D_θ^{-1} and helical regime $r_L(E)/c$ become equal, acceleration energy reaches maximum,

$$E_{\max} \approx \left(\frac{\Gamma_{\rm sh}}{100}\right)^2 \left(\frac{\lambda_d}{10c/\omega_{\rm pp}}\right) \left(\frac{\sigma_d}{10^{-2}}\right) \left(\frac{\sigma_u}{10^{-8}}\right)^{-1/2} \ \mathrm{PeV},$$

where $\sigma = B^2/4\pi n m_p c^2$ is magnetization, λ is scattering scale.
The authors conclude :**“Ultra-relativistic shocks are disfavoured as sources of high energy particles, in general.”**

TOPOLOGICAL DEFECTS

Symmetry breaking in early universe results in phase transitions (D. Kirzhnitz 1972), accompanied by TDs (T. Kibble). TDs are formed at the boundary of two domains (horizons) with different directions of symmetry breaking. Their common feature is production of HE particles.

Ordinary strings

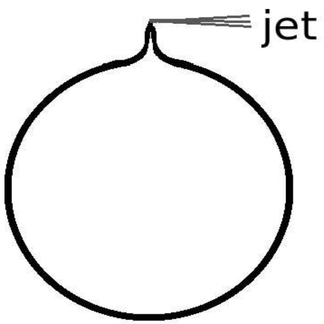

Produced at $U(1)$ symmetry breaking as $< \phi >= \eta \exp i\theta$.
η determines the thickness of the string $d \sim \eta^{-1}$, e.g. 10^{-30} cm at $\eta \sim 10^{16}$ GeV. The strings exist in the form of endless strings and closed loops. They have tremendous tension $\mu = \eta^2$, due to which a loop oscillates and produces a cusp at each period. It moves with very high Lorentz-factor above $\Gamma \sim 10^{10}$.
Particles are massless inside the string and massive outside.
Particles escaping from cusp segment have $E_{\max} \sim \Gamma_c \eta$,
Particles are emitted as jets with opening angle $\theta \sim 1/\Gamma_c$.

SUPERCONDUCTING STRINGS

In a wide class of particle models strings are superconducting (Witten 1985). Consider a string with electric field and **fermions** as charge carriers.

$\frac{dp}{dt} = e\mathcal{E}$, $p_F = e\mathcal{E}t \sim m_X$, (exit), $n_X = \frac{p_F}{2\pi} = \frac{e\mathcal{E}t}{2\pi}$,

$J = en_X c = \frac{e^2\mathcal{E}t}{2\pi}$, $\frac{dJ}{dt} = e^2\mathcal{E}$, (superconductivity)

Electric field appears as $\mathcal{E} \sim Bv$, when a string moves through magnetic field B, e.g. in galactic cluster with $B \sim 1\ \mu$G, and thus $J \sim e^2 vBt$.

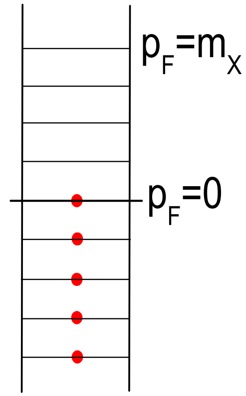

UHE neutrino jets from superconducting strings

V.B., K.Olum, E.Sabancilar and A.Vilenkin 2009

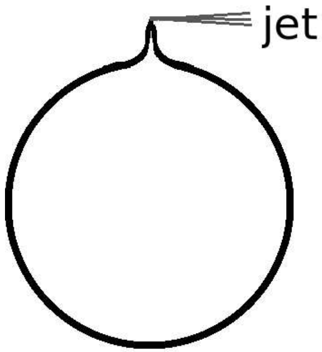

Symmetry breaking scale: $\eta \gtrsim 1 \times 10^9$ GeV.

Lorentz factor of cusp $\gamma_c \sim 1 \times 10^{12} \eta_{10}^{-1} B_{\mu G}^{-1}$,

Clusters of galaxies dominate in current generation.

Energy of ejected particles $E_X \sim \gamma_c \eta \sim 10^{22}$ GeV.

CONCLUSION on TOPOLOGICAL DEFECTS

- **Existence of TDs is a robust cosmological prediction. They are not yet found because they were searched for in the wrong place and in the wrong range of parameters.**

- **Production of UHE particles is a common feature of TDs. They are produced even by ordinary strings at self-intersection, but in most cases the fluxes are small. The produced UHE particles are protons, photons and neutrinos, but not UHE nuclei, as observed in Auger.**

- **TDs naturally produce particles with energy higher than 10^{20} eV, while these energies remain the serious problem for astrophysical accelerators.**

- **There is impressive progress in theoretical study of HE radiation from ordinary strings which are the simplest TDs. The predictions directly follow from fundamental properties of the strings: existence of cusps. gravitational interaction of intermediate particles (higgses, dilatons and moduli) with a string field Φ and basic string parameter $\eta^2 = \mu$, satisfying $G\mu \gtrsim 10^{-20}$, while the present observational limit is $G\mu \lesssim 10^{-6}$.**

SUPERHEAVY DARK MATTER (SHDM)

Galaxy formation starts at **inflation**, maybe DM too?

- **Production mechanism:**
  Most natural and attractive one is creation of particles in time-varying gravitational field at **inflation**, No coupling with inflaton, X can be sterile.

$$\mathcal{L} \sim (1/2)\xi \, R \, X^2$$

  where $\xi = 1/6$ is conformal coupling of **X** with space-time curvature **R**.
  Creation occurs when $H(t) \sim M_X$, and since $H \sim m_\phi \sim 10^{13}$ GeV.

$$m_X \sim 10^{13} \text{ GeV},$$

  e.g. $m_X \sim (2-3)10^{13}$ GeV results in $\Omega_X h^2 \sim 0.1$ (WMAP).

- **Accumulation in halo** is gravitational effect, which does not depend on m_X**:**

$$\frac{n_X^{\rm halo}}{n_X^{\rm ext}} = \frac{\rho_{\rm cdm}^{\rm obs}}{\Omega_{\rm cdm}\rho_{\rm cr}} = 2.1 \times 10^5$$

- **Lifetime $\tau_X > 10^{10}$ yr**
  is provided by discrete gauge symmetry. This symmetry is very weakly broken by quantum gravity effects (wormhole) :

$$\mathcal{L} \propto \frac{1}{m_{\rm Pl}} X\phi^3 \exp(-S),$$

  where S is wormhole action, e.g. $S = 8\pi^2/g_{\rm str}^2$. Due to this effect, X decays to any partons , which initiate then the parton cascade. At confinement distance the partons turn into hadrons, and final particles are protons, pions and kaons. Photons, neutrinos and electrons are produced in pion decays. The photon/proton ratio is of order 2 - 3. The energy spectrum is $E^{-1.9}$.

- **Particle candidates:**
  Many candidates for long-lived superheavy particles are found in string models, in some discrete Z_N models, in QCD-like $SU(N_c)$ and Kaluza-Klein models and others. The most known particle of such kind is crypton from a hidden sector of string theory (J.Ellis et al 1999).

- **Pioneering works** on SHDM includes: Kuzmin and Rubakov 1997,
  V.B, Kachelriess, Vilenkin 1997, Kolb et al 1997, Kuzmin and Tkachev 1998.

UHECR: propagation, signatures and mass composition

Spectrum and Features

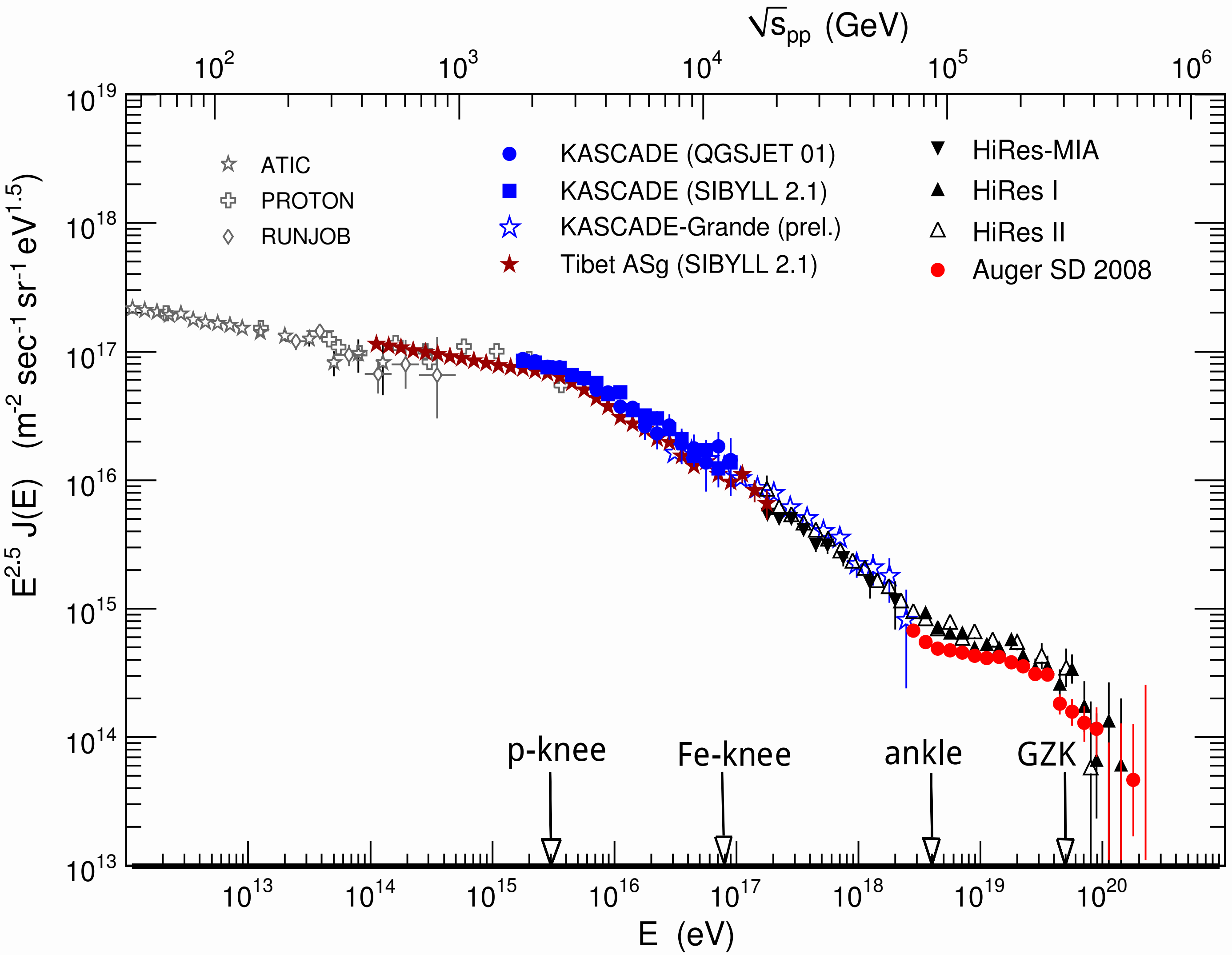

IRON KNEE and ANKLE

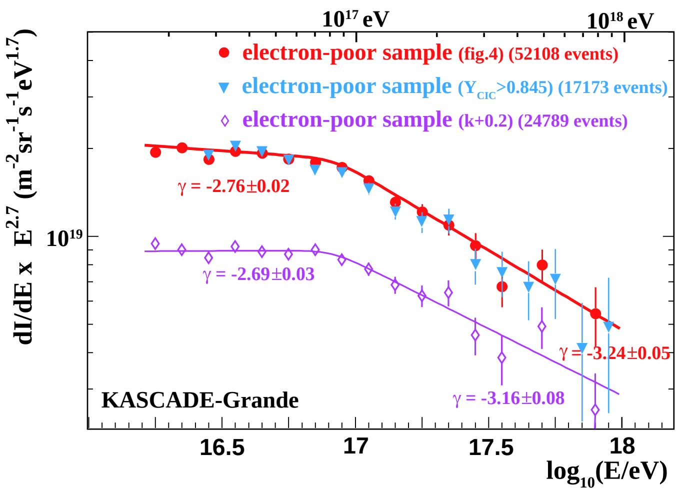

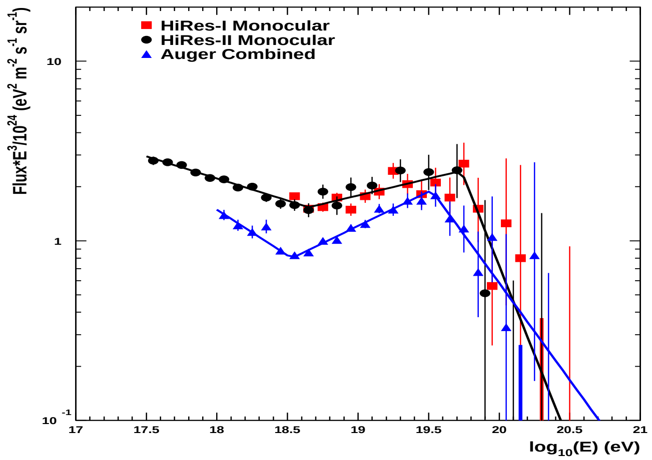

Observed Iron knee and ankle in power-law approximation

Kascade-G : $E_{\rm knee}^{Fe} \approx 80\ \ \mathrm{PeV}$

.

.

HiRes : $E_a = 4.5 \pm 0.5\ \ \mathrm{EeV}$

TA : $E_a = 4.9 \pm 0.3\ \ \mathrm{EeV}$

Auger : $E_a = 4.2 \pm 0.1\ \ \mathrm{EeV}$

Ankle can be explained as:

- **Transition** from galactic to extragalactic CRs
- intrinsic feature of **pair-production dip**

ANKLE is not a feature of transition

- At $1-4$ EeV, i.e. below the ankle, the mass composition according to all three detectors, Auger, TA and HiRes, is presented by protons (p) or **p + He**.
- In ankle model these particles are galactic.
- The measured anisotropy (Auger 2011) and MC simulations exclude galactic protons below ankle, and thus ankle is excluded as transition from galactic to extragalactic CRs.

Where is the transition ?

KASCADE-Grande found the light component with the following properties:

- p+He component at 0.1 - 1.0 EeV separated as 'electron-rich'
- extragalactic, otherwise anisotropy at $E \sim 1$ EeV.
- flat spectrum $\gamma = 2.79 \pm 0.08$, cf $\gamma = 3.24 \pm 0.08$ for total.

Hidden ankle transition

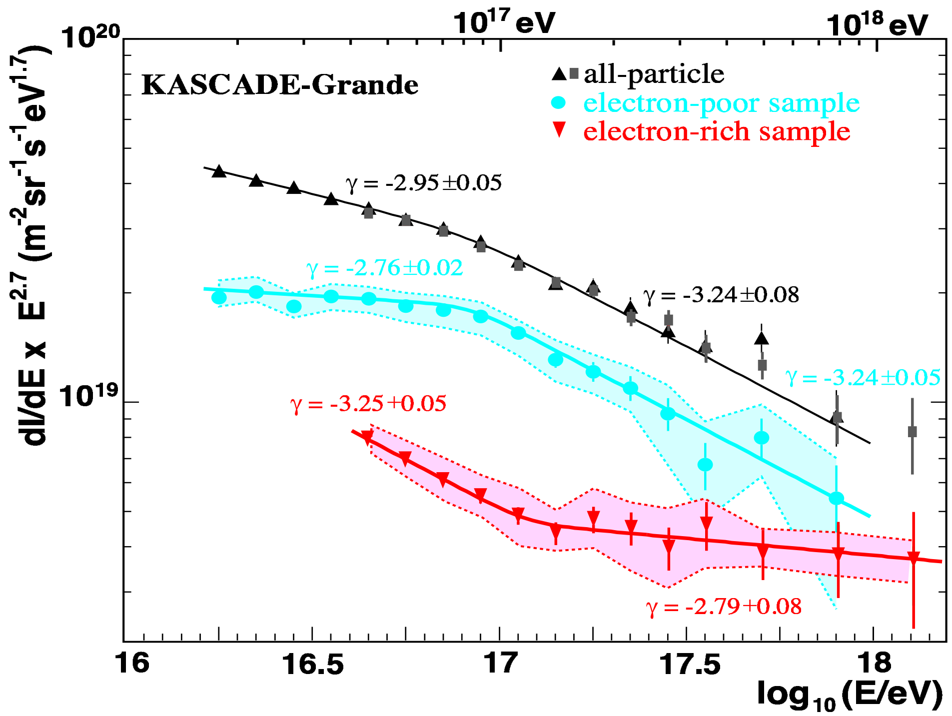

PROPAGATION and SIGNATURES

Signatures of particle propagation through CMB and EBL

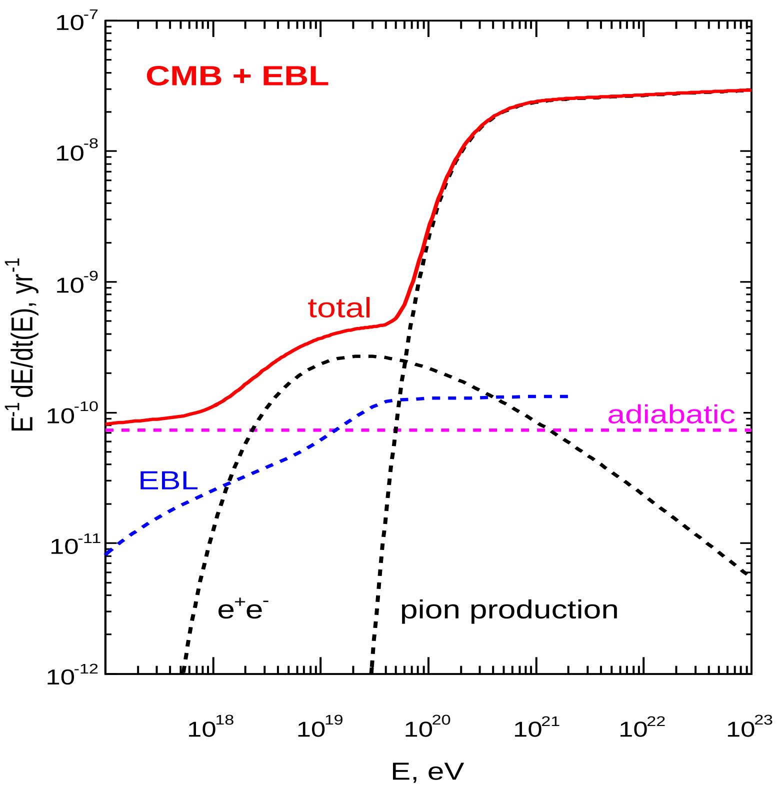

$$E_{\rm eq1} = 2.4 \times 10^{18}\ \text{eV}, \quad E_{\rm eq2} = 6.1 \times 10^{19}\ \text{eV}$$

Pair-production dip and GZK cutoff.

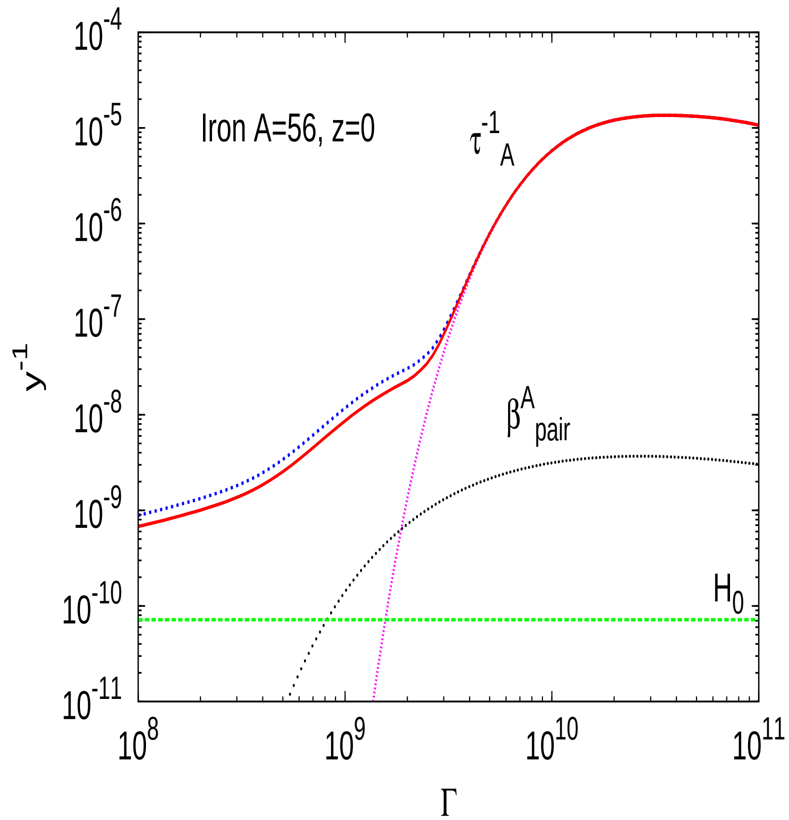

Nuclei photo-dissociation: GR cutoff 1961.

$$\tau_A^{\rm ebl}(\Gamma_c) = \tau_A^{\rm cmb}(\Gamma_c)$$

$$\Gamma_c = 3.2 \times 10^9, \quad E_c = 1.8 \times 10^{20}\ \text{eV}$$

•

UHE protons

INTERACTION SIGNATURES AND MODEL-DEPENDENT SIGNATURES

We want to see **observational signatures of interaction**, but in our calculations **model-dependent quantities** also appear, such as **distances** between sources, their cosmological **evolution**, modes of **propagation** (from rectilinear to diffusion), local source **overdensity** or **deficit** etc.

Energy spectrum in terms of **modification factor** characterizes well the **interaction signatures**.

MODIFICATION FACTOR

$$\eta(E) = \frac{J_p(E)}{J_p^{\rm unm}(E)}$$

where $J_p^{\rm unm}(E) = KE^{-\gamma_g}$ includes only adiabatic energy losses. Since many physical phenomena in numerator and denominator compensate or cancel each other, dip in terms of modification factor is less model-dependent than $J_p(E)$.

It depends very weakly on:
γ_g and $E_{\rm max}$,
modes of propagation (rect. or diff.),
large-scale source inhomogeneity,
source separation within 1-50 Mpc,
local source overdensity or deficit,..
It is modified by presence of nuclei ($\gtrsim 15\%$).
Experimental modification factor:
$\eta_{\rm exp}(E) = J_{\rm obs}(E)/KE^{-\gamma_g}$.

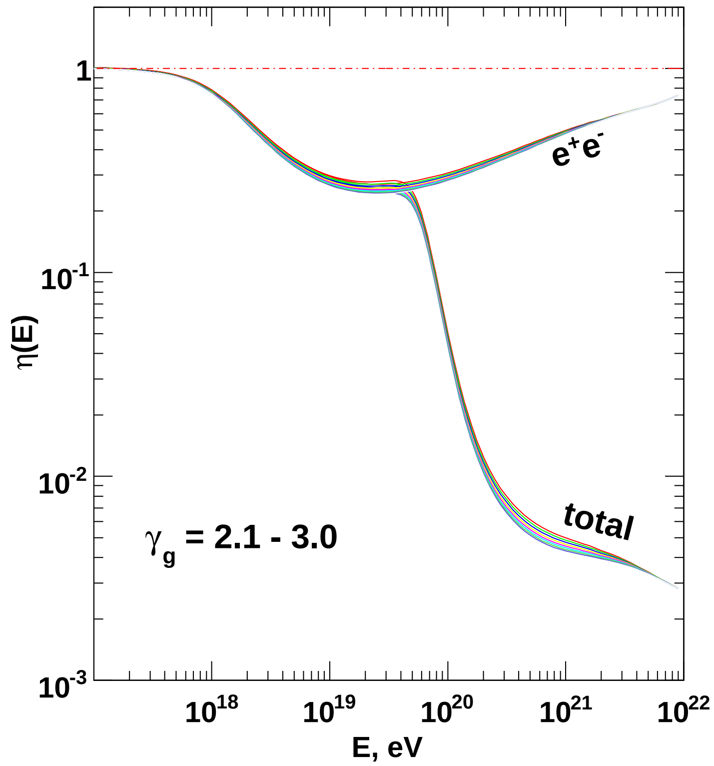

Comparison of pair-production dip with observations

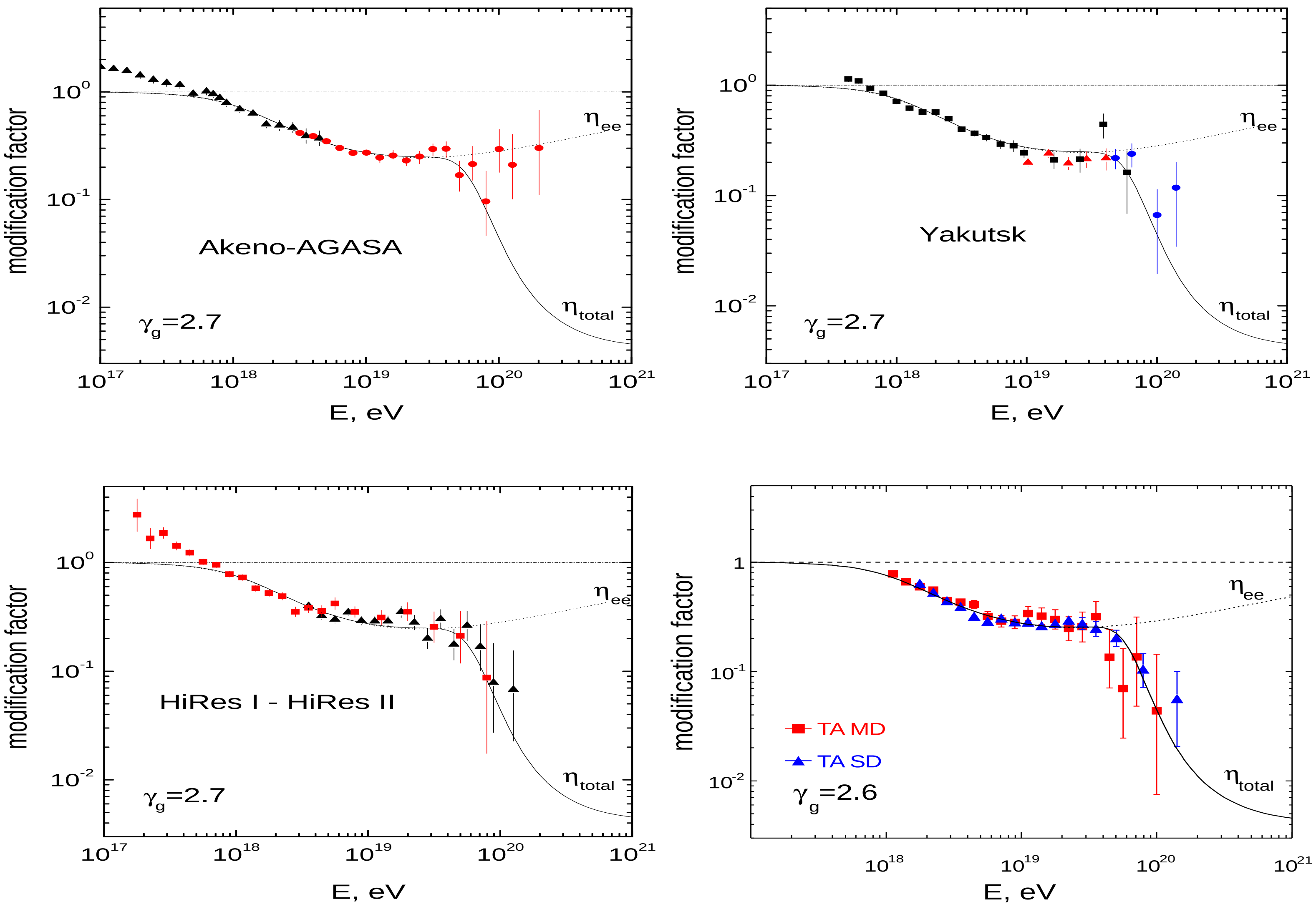

GZK CUTOFF IN AUGER SPECTRUM 2007

(combined and hybrid events)

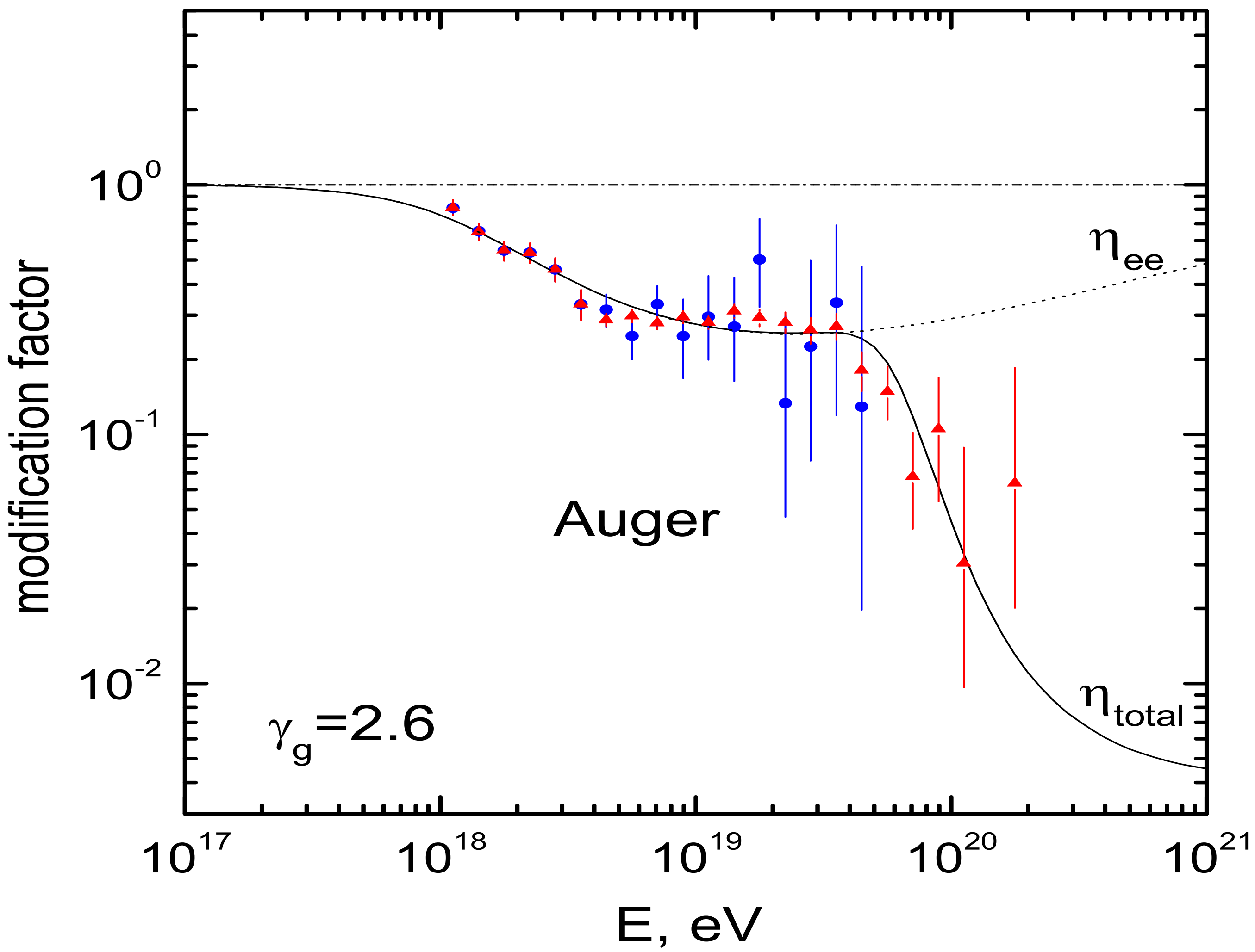

GZK CUTOFF IN AUGER SPECTRUM 2015

(combined and hybrid events)

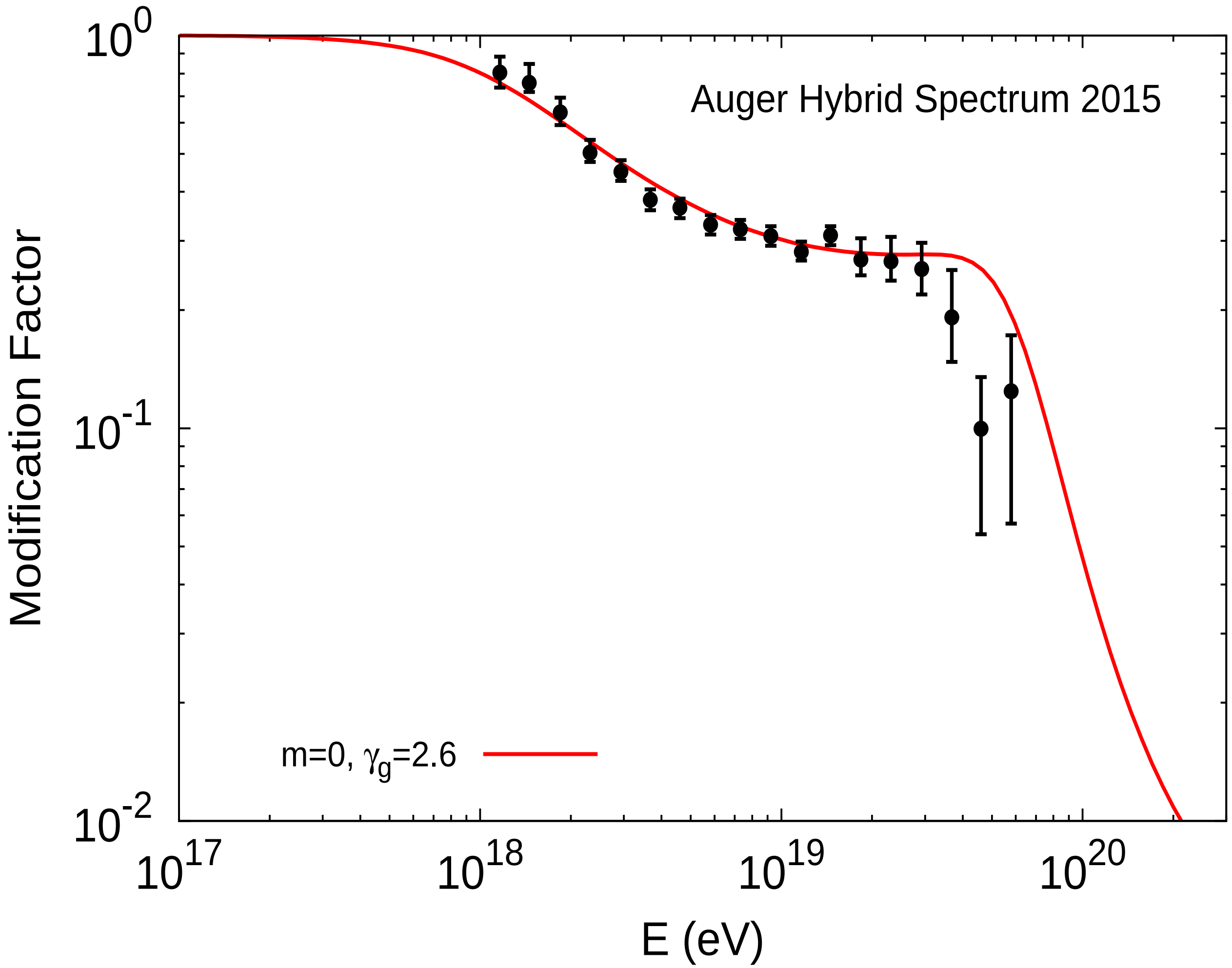

GZK CUTOFF IN TA SPECTRUM 2015

(combined and hybrid events)

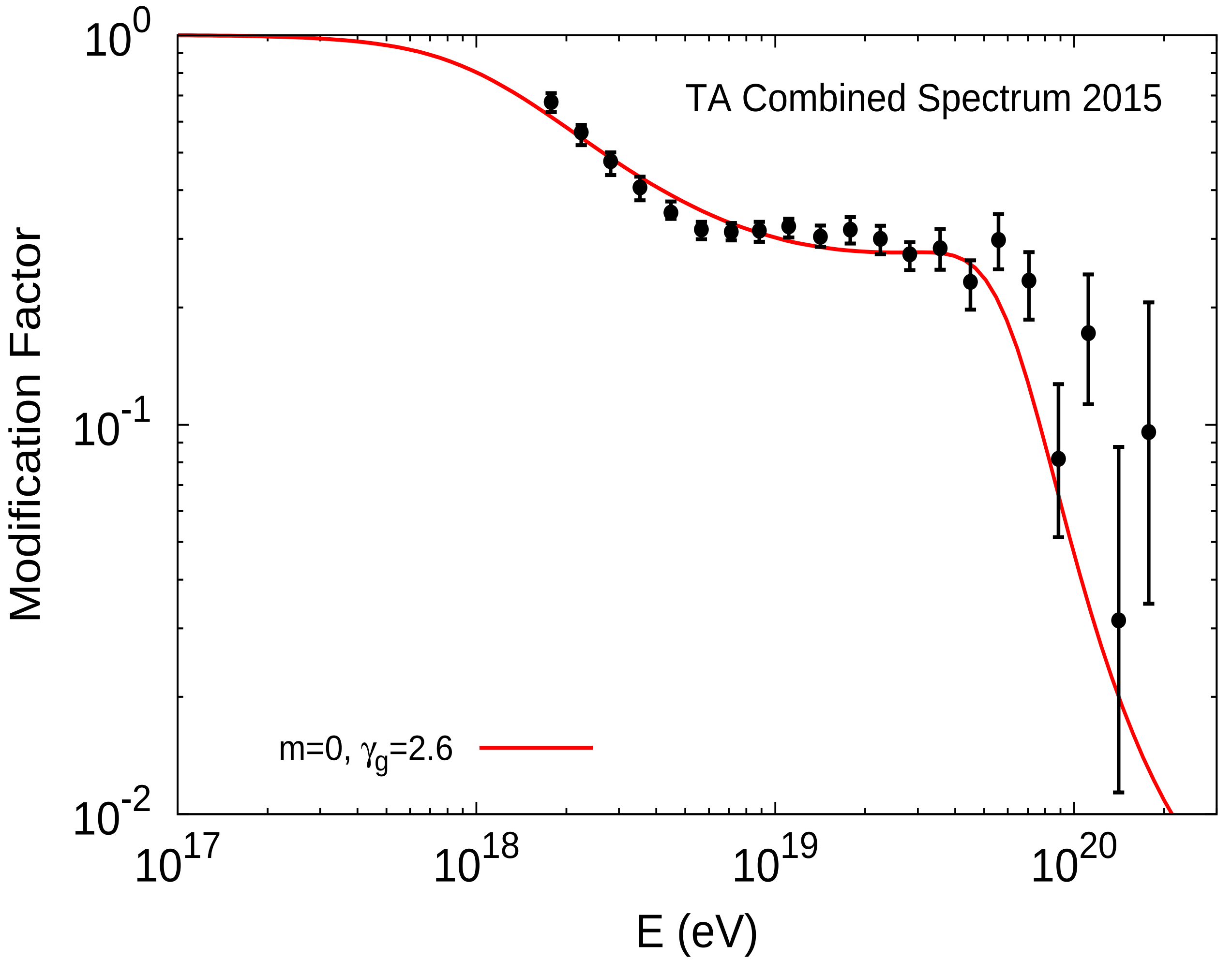

MASS COMPOSITION

MASS COMPOSITION: HIRES (top) vs AUGER (bottom)

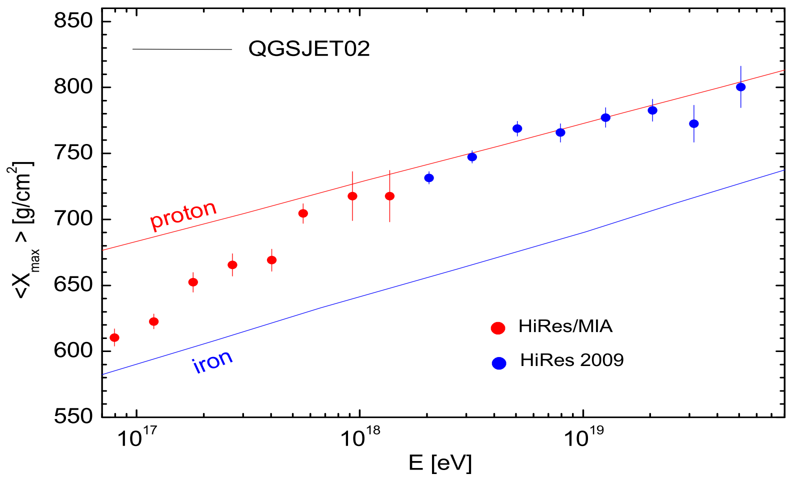

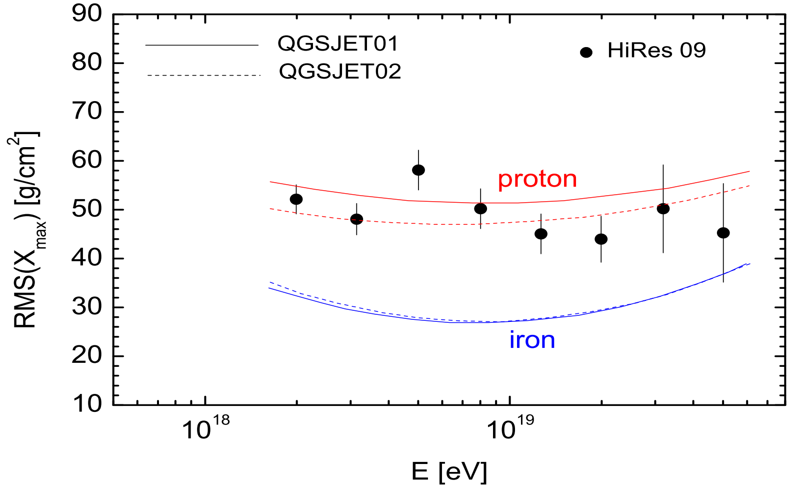

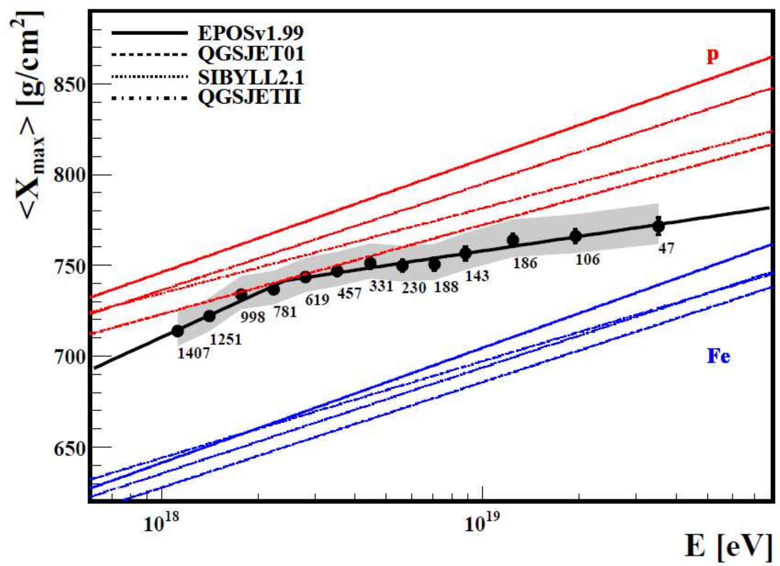

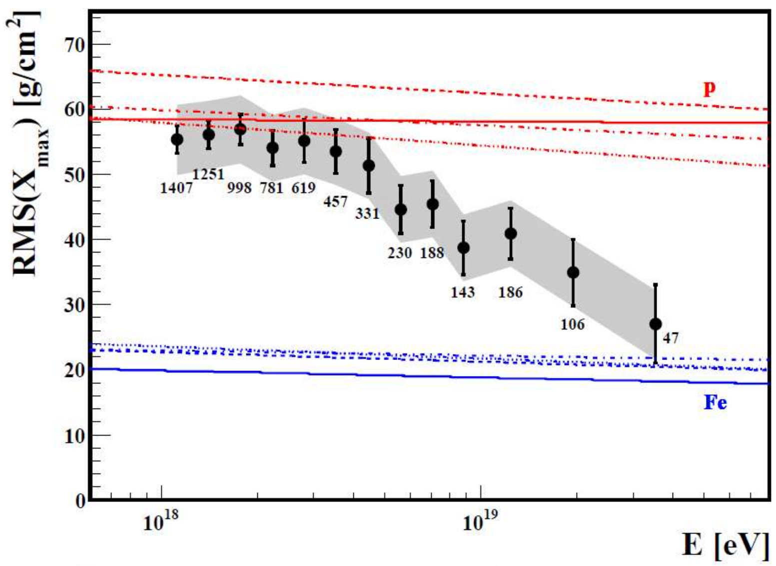

$X_{\max}$ and RMS of Auger are confirmed by $X^{\mu}_{\max}$ and $\theta_{\max}$ data.

SHAPE-FITTING ANALYSIS OF AUGER MASS-COMPOSITION

Determination of mass composition using $\langle X_{\max}\rangle$ (the mean value) and RMS (dispersion) is not precise and suffers degeneracy: quite different mass compositions may have the same $\langle X_{\max}\rangle$ and RMS. Auger collaboration developed the method of shape-fitting analysis of distribution of showers.

$$N(X_{\max}, E)$$

The method consists in the following steps:

First collect the huge statistics of the cascade shapes from measurements of fluorescent light,

$$N_{part}^{cas}(X, E)$$

and build from them $N(X_{\max}, E)$ distributions for fixed energies E.

The mass composition of UHECR is described by the four discrete nuclei: p, He, N, and Fe.

Use the cascade shapes from measured fluorescent light.

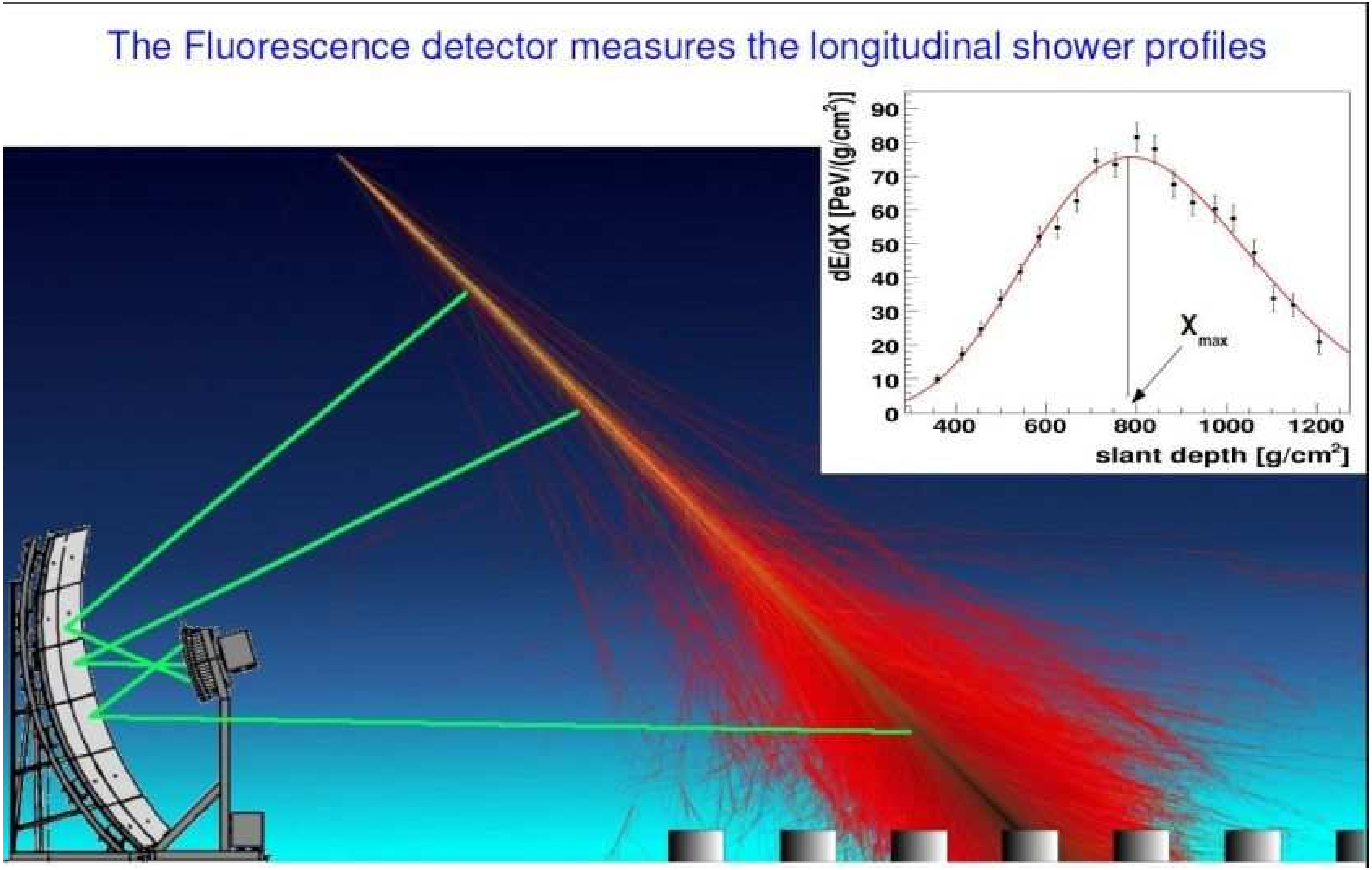

The Auger 2014 shape-fitting method.

- Create template of theoretical MC distributions $N_{A,E}(X_{\max})$ for the same E using three models of hadron interactions (EPOS, QGSJet and Cybill).
- Choose the set of **measured** distributions $N_{\rm obs}(X_{\max})$ for the same E and ΔE, as in measured distributions .
- First fit $N_{\rm obs}(X_{\max})$ by linear superposition of **two** theoretical distributions $N_i(X_{\max})$, i=p, Fe, for the same E and ΔE.
- Add next **He** and then **N** nuclei.
- The quality of fit is characterised by **p-value**, with $p = 1$ maximum value, $p < 0.1$ for the bad fit, $p < 10^{-3} - 10^{-4}$ for excluded case.

Iron and Proton fractions

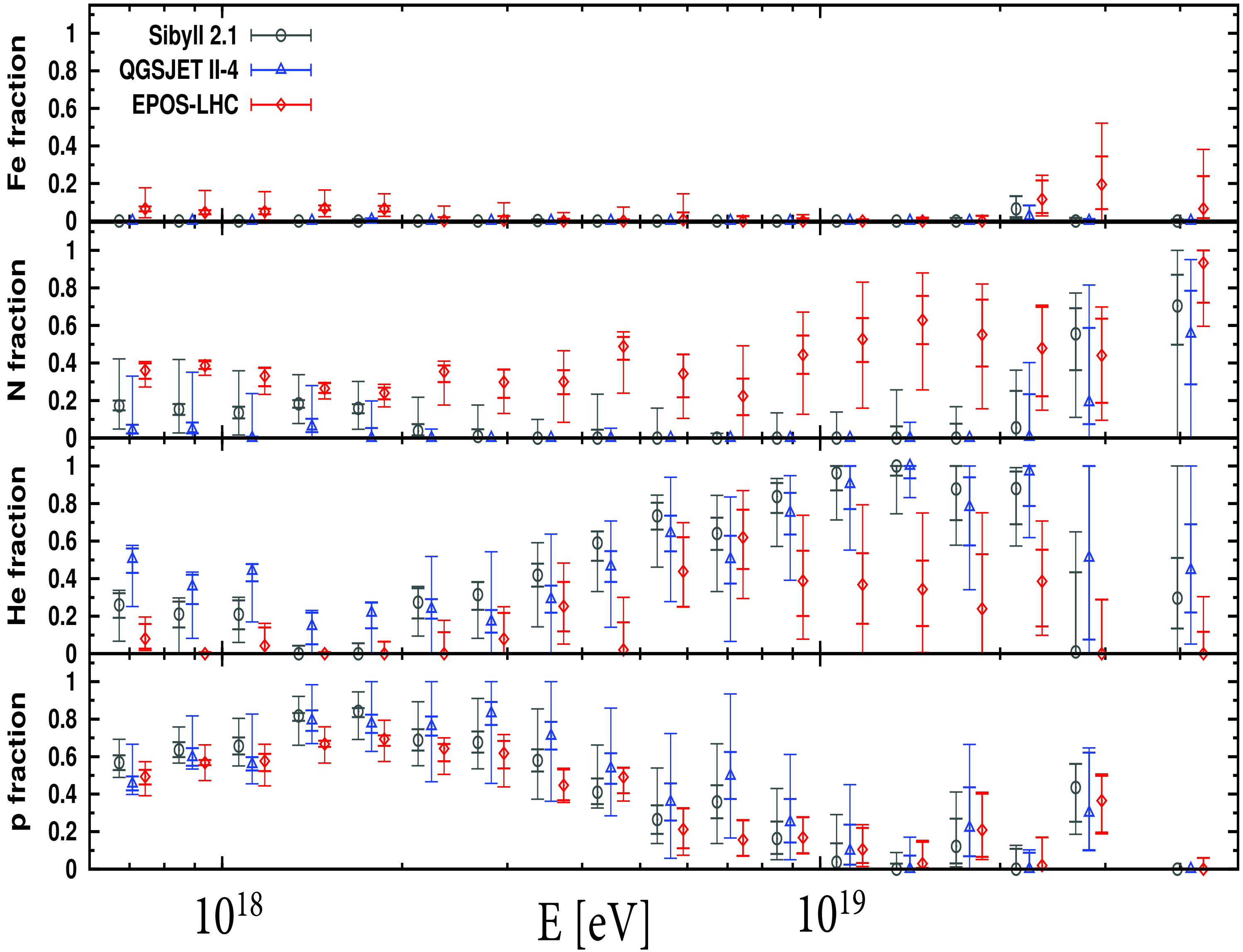

. shape-fitting analysis agrees with zero fraction of Iron.

p+He model

based on shape-fitting Auger analysis

R. Aloisio and VB, arXiv 1703.0867

p+He (for QGSjet and Sybill) saturates the total observed flux.

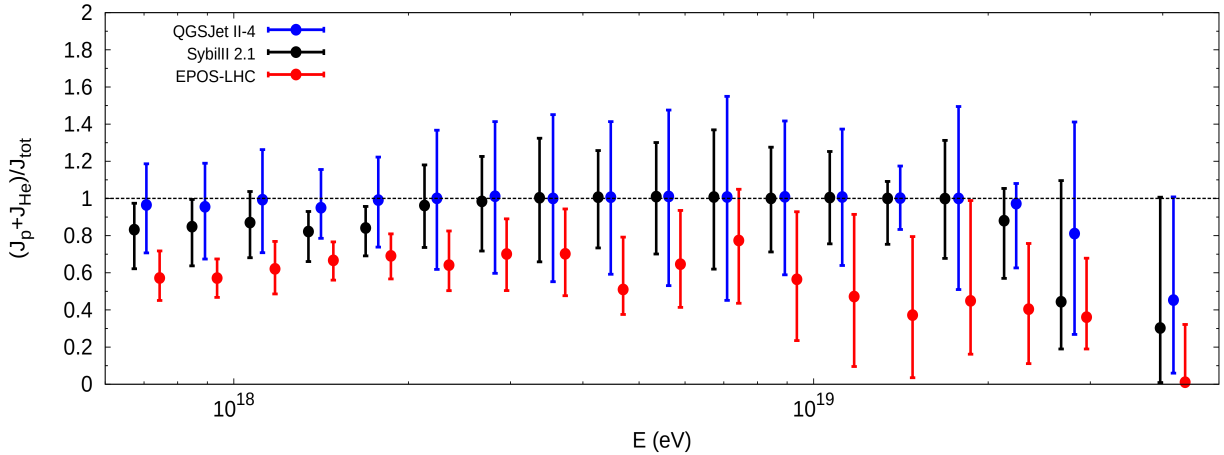

. The basic assumption of the model:

existing detectors do not distinguish reliably He from protons.

It implies p+He as one component, with He/p ratio as a free parameter.

Energy spectra in p+He model for Auger and TA with ratio $He/p = 0.35, \quad \gamma_g = 2.2$ and $E_{\max} = 8 \times 10^{19}$ eV.

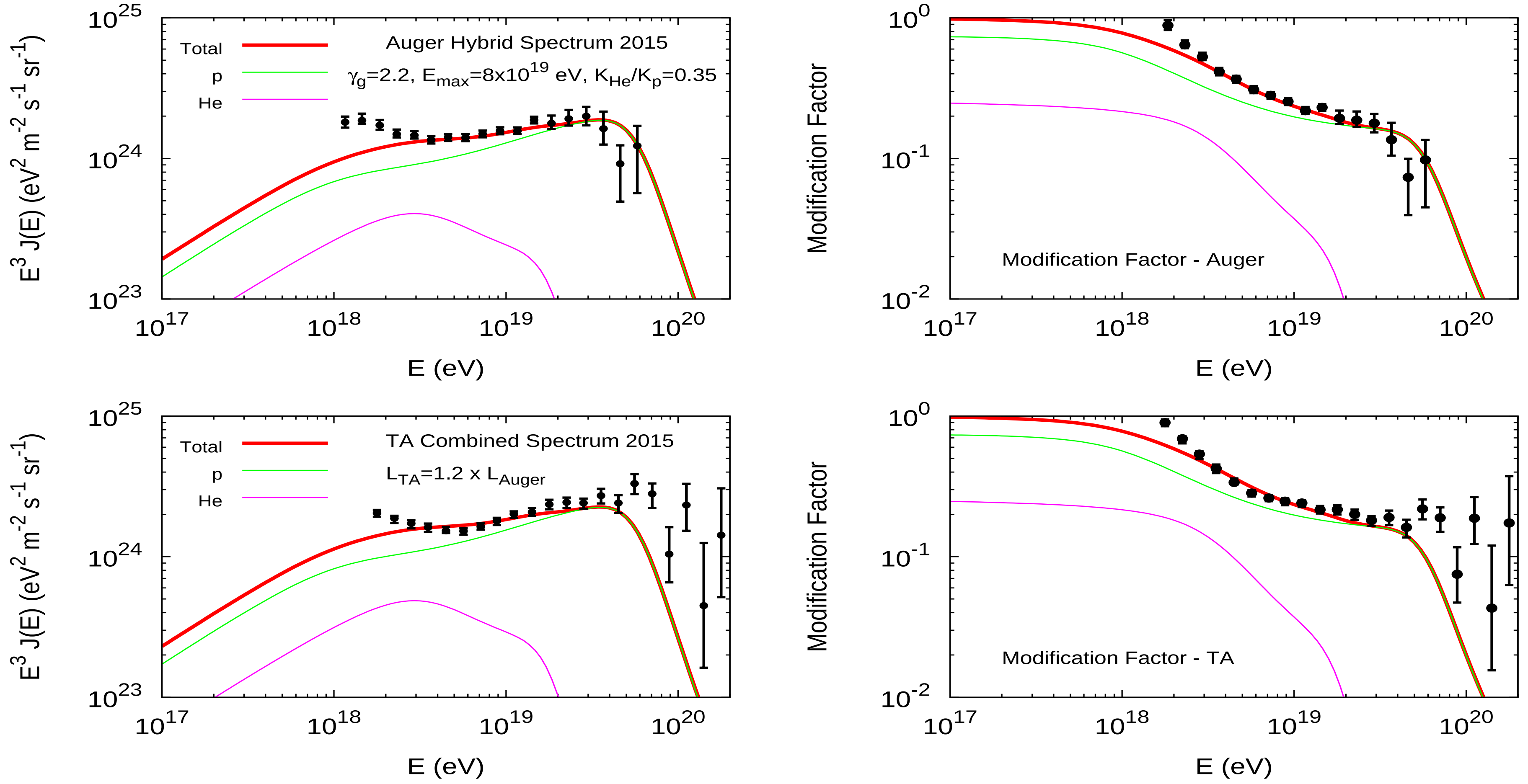

To analysis of Joint Group